Optimal Planning of a Multi-Carrier Microgrid (MCMG) Considering Demand-Side Management

Vahid Amir *, Shahram Jadid **‡, Mahdi Ehsan ***

* Department of Electrical Engineering, Faculty of Electrical Engineering, Science and Research Branch, Islamic Azad University, Tehran, Iran.

** Department of Electrical Engineering, Faculty of Electrical Engineering, Iran University of Science and Technology, Tehran, Iran

*** Department of Electrical Engineering, Faculty of Electrical Engineering, Sharif University of Science and Technology, Tehran, Iran.

(V.amir@iaukashan.ac.ir, jadid@iust.ac.ir, ehsan@sharif.edu)

‡ Corresponding Author; Shahram Jadid, Electrical Eng. Department – Iran University of Science & Technology, Narmak – Tehran – Iran, Tel: +98 2177491223, jadid@iust.ac.ir

Received: 24.06.2017 Accepted:07.08.2018

Abstract- The multi-carrier microgrid (MCMG) is a restricted district comprising convertors and energy storage systems (ESSs) that are used to fulfill various energy demands. The structure and optimal operation of these MCMGs with regard to fulfilling multi-carrier demands are presented in relation to their rapid spread. In this paper, a two-stage optimum planning and design method for an MCMG is presented in the planning horizon. The investment and operation (fuel and maintenance) costs are considered concurrently to find the optimal type and size of components over the planning horizon. At the first stage, the genetic algorithm (GA) is applied to determine the optimal type and size of components, such as combined heat and power (CHP), boiler, transformer, and solar panels. At the second stage, the mixed-integer nonlinear programming (MINLP) technique is used and simulated by the GAMS software to solve the operational problem with regard to the forecasted energy demands. This method is examined on a typical MCMG and the effectiveness of the proposed method is proven.

Keywords Cooperative operation; Demand response (DR); Genetic algorithm (GA); Multi-carrier microgrid (MCMG); Planning.

1. Introduction

Nowadays, various energy carriers—for example, carriers of electricity, natural gas, and heat—are supplied by autonomous infrastructure. Simultaneous integration and analysis of the infrastructure is indispensable due to the wide-ranging utilization of small-scale energy resources (SSERs), especially natural gas-fired generations, such as combined heat and power (CHP) [1,2] and combined cooling, heating, and power (CCHP) [3, 4].

So far, only rare studies have paid attention to the integrated energy system, which includes multi-carrier microgrids (MCMGs), hybrid energy hubs (EHs), and EHs [5], instead of focusing on a single carrier. Microgrids (MGs) include several energy carriers that are known as small-scale energy zones (SSEZs) or MCMGs [6]. The United States Department of Energy has defined the MG as a group of interconnected loads and distributed energy resources (DERs) with clearly defined electrical boundaries that act as a single controllable entity with respect to the grid, and that can connect or disconnect from the grid to enable it to operate in both grid-connected or island modes [7]. The simultaneous inspection of carriers and sources in an MCMG offers a number of potential advantages, such as increasing the flexibility of the energy requirement, the improvement in local reliability [8], the synergy effects of different energy carriers, low operational costs, power quality enhancement and emission [5,10–13].

In fact, the key idea of an MCMG is to link different energy sources using current energy infrastructures in a limited district while the required demand is satisfied. Some examples of real facilities that can be modeled as an MCMG include the supply of industrial plants (steel work, paper mills), big building complexes (airports, shopping malls, and hospitals) and power plants (co- and tri-generation) [14].

In previous works, simultaneous operational and planning optimization, especially in MCMGs, has been rarely reported. The expansion planning of an energy system is mainly discussed in the context of optimal size and type determination, location, and time of components installation over a planning horizon [15], whereas the planning is classified into static, quasi-dynamic, and dynamic [16,17].

In conventional studies, the expansion planning of sources was performed under the influence of a single energy carrier. As is known to all, reasonable planning is an important premise and a guarantee for the stable and efficient operation of MCMGs. So, in order to achieve an optimal situation for satisfying the demand, the optimal, simultaneous operation and planning of these MCMGs is unavoidable, whereas the various energy infrastructures are coupled and have interchanges.

The EH approach is employed and presented in many papers [1,15]. In fact, the MCMG as a sample structure of the EH with the goal of integrating various energies has been studied in a few papers [18–20]. Most of the reported literature in this area is focused on operational optimization; the focus is not on component selection or their size. The discussions mainly pay attention to different operational issues in multi-carrier energy (MCE) systems, such as economic dispatch [21–23], optimal gas and power flow [23–25], unit commitment [26,27], and the optimal coupling of energy carriers [28,29].

A few works have studied the structural issues in MCE systems up until now. For instance, the expansion planning of an electric and natural gas network on the market environment is discussed in [30]. On the other hand, the optimal size determination of co- and tri-generations, such as CHP and CCHP, as one of the main components of MCE systems, is accomplished in [31,32], respectively. Several components in MCE systems are considered and sized optimally from different objective function (OF) viewpoints, such as cost, efficiency, and emission, in literature [8,16,31,33,34]. The reliability indices for designing MCE systems are investigated and computed in a few papers [8,35]. The optimal load supplement in an MCE system depends not only on the proper operation of the components but also on the design of the system. So, simultaneous operation and planning of MCE systems is required [26]. CHP and CCHP in a typical MG are sized optimally along with the cooperative operation [36–38]. The operation and planning of an EH system is carried out simultaneously along with the reliability constraints in [15]. Here, the reliability is handled within the optimization process and not afterward, leading to the possibility of designing a hub with a predetermined level of reliability for supplying loads.

In Ref. [26,39], the operational optimization of an EH system along with the optimal sizing of an electrical storage system is carried out in nonlinear programming (NLP), whereas different elements, such as electrical and thermal storage, and convertors, are selected and sized optimally inside an EH system in [39]. A developed, entirely linearized model of the aforementioned paper is proposed in [40]. The fast convergence and a better optimal performance are derived in this model, and the optimization problem is solved using the GAMS software. The General Algebraic Modeling System (GAMS) is a high-level modeling system for mathematical programming and optimization. GAMS is tailored for complex, large scale modeling applications, and allows you to build large maintainable models that can be adapted quickly to new situations. Likewise, the optimal sizing of a backup storage system is planned along with reliability indices in an electrical MG [41]. Embedded storage offers advantages, such as the effective usage of DERs, volatility mitigation, reduction of harmonic and intermittency problems of renewable energy resources, voltage and frequency stability, peak load management, power quality improvement, better control, and deferment of system upgrades [42]. Considering the aforementioned research studies, the long-term planning and short-term operation of selected components in an MCMG have not been reported concurrently, while the various energy infrastructures are coupled with the system containing an electric and natural gas network.

Hence, in this paper, a two-stage optimal method is proposed. At the first stage, static design optimization is performed to obtain the optimal type and capacity of components—specifically, mounted energy storage systems (ESSs) along with their investment costs, with a genetic algorithm (GA) for the planning horizon. At the second stage, the operational optimization of selected components is carried out to calculate the optimal strategy using the mixed-integer nonlinear programming (MINLP) algorithm via the GAMS software. Chronologically, load curves are utilized for electric and heat demands in addition to two typical days for two typical months. The typical days for their seasons are classified according to weekdays and weekends for two different months.

A two-stage optimum planning and design method for an MCMG is presented in the planning horizon. Since the loads are classified into responsive and non-responsive, the effectiveness of the existing controllable loads in planning the proposed MCMG with a novel approach of the demand response (DR) program is investigated.

The main contributions and innovation of this paper are briefly summarized as follows:

1. Modeling the optimal structure of the system (selection and optimal sizing of elements such as CHP, boiler, transformer, and photovoltaic [PV]), along with the operational optimization problem.
2. Proposing a novel approach of the DR program in the planning problem.
3. A two-stage optimum method to solve the co-optimization problem.

2. Problem Description

The MGs will comprise various energy carriers known as MCMGs, as shown in Fig.1 The optimal supply of various loads in an MCMG depends not only on the proper operation of the components but also on the structure of these systems. Hence, in order to have a significant cost reduction for load requirements, the design of different structures in an MCMG, along with its operation, needs to be performed. The rest of this section is divided into two subsections. The first subsection discusses a typical MCMG while the second describes the planning problem of these systems, considering DR programs.

2.1. Typical MCMG

An MCMG is formed of a low- or medium-voltage energy network, including electricity, natural gas, and heat. In other words, energy conversion is possible through some components, such as transformers, heat exchangers, co- and tri-generation, and other energy convertors. Besides the convertors, DERs like ESSs and renewable energy resources (RERs) can satisfy demand and effect a significant reduction in energy cost with regard to the time-of-use (TOU) carrier's prices. A DR program can provide more flexibility to the network for meeting the demand in the given period. In this paper, an MCMG with coordination among its components to fulfill multiple energy demands for 24 hours is modeled for the test case of the MCMG structure. This is depicted in Fig.2.

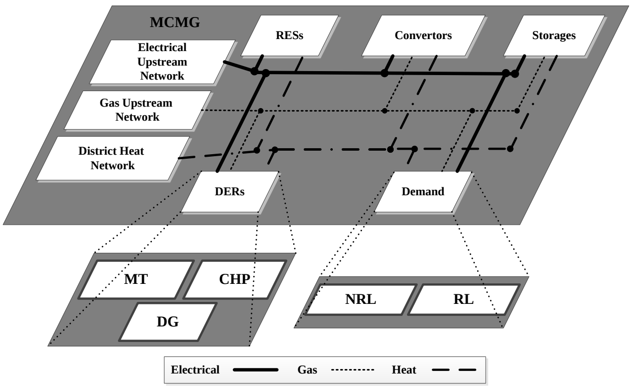

Fig. 1. MCMG structure†.

† In Fig 1, RL and NRL are the abbreviation for responsive and non-responsive loads, respectively.

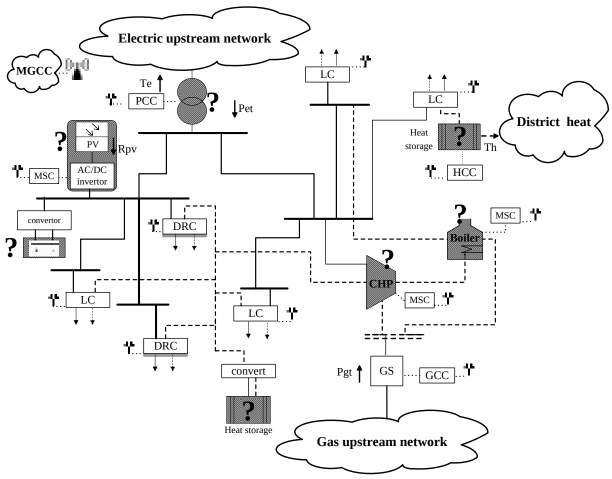

Fig. 2. A test case of the MCMG structure.

2.2. Proposed MCMG Designing

The optimal type and capacity, location, and time for the installation of each component are taken into account for the planning problem in case the loads are optimally fulfilled. Therefore, in order to search for and assess appropriate sizes and types of available components inside an MCMG, as shown in Fig.3, it is binding to draw a realistic model and an optimal solution method. In this paper, an MCMG in a single-bus mode is drawn for the planning problem, for which the availability of a transformer, CHP, boiler, and PV are considered ideal. In addition, an ESS with a specified capacity is embedded inside the proposed MCMG. The main goal is to select the best components, whereas the static planning is targeted.

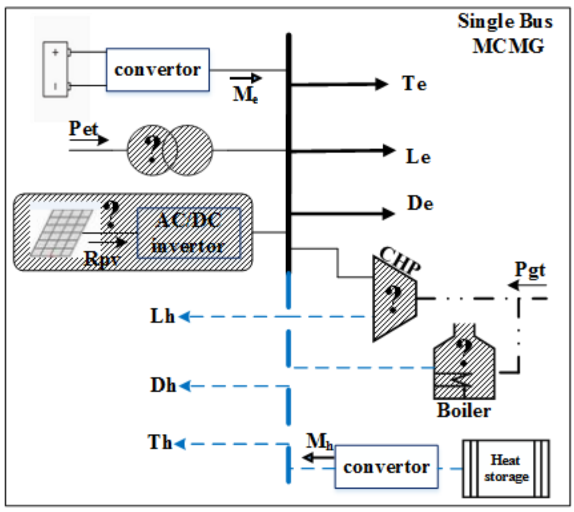

Fig. 3. Desired MCMG for structural and operational optimizations.

3. Model Outline

As the transmission lines are considered capable of ensuring the maximum flow of energy in this model (represented as an MCMG), the selection and commitment of different possible components inside the MCMG and the quality of their operation are considered as a single-bus system, which is depicted in Fig.3. The MCE system is used to model the proposed MCMG. The MCE system, as is apparent from its name, is a system that surrounds various energies and energy interactions in addition to energy saving are conceivable inside it [43]. Fig.4 shows a hybrid EH system. The main aim of static planning in this work is to choose the best components while the equality and non-equality constraints are satisfied. The proposed MCMG is in the grid-connected mode, as seen in Fig.3. Moreover, electricity purchase and sale from or to the upstream network is feasible while the surplus heat can be sold to the district heat network.

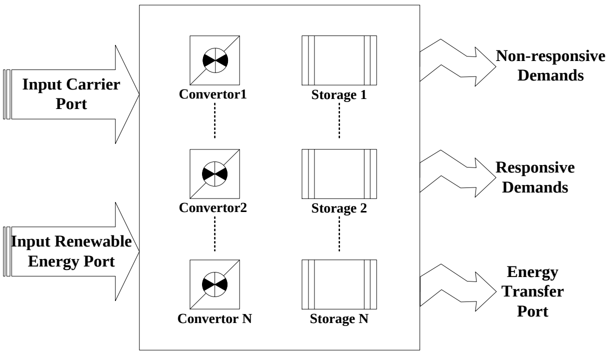

Fig. 4. Simplified figure of analyzed MCMG (represented as EH).

The non-responsive and responsive loads for the planning horizon are defined below.

$$L_l(y,m,d,t)=\sum_{lo=1}^{Nl_{lo}} L_{l,lo}(y,m,d,t) \quad l\in\{e,h\} \tag{1}$$

$$D_l(y,m,d,t)=\sum_{lo=1}^{Nd_{lo}} D_{l,lo}(y,m,d,t) \quad l\in\{e,h\} \tag{2}$$

3.1. EH System Modeling

The proposed MCMG is modeled as a single-bus system and defined as an EH system. The matrix's model of energy balancing in input and output hub ports based on installed components at given intervals is represented as:

$$L(y,m,d,t)+D(y,m,d,t)+T(y,m,d,t)=Co\times \begin{bmatrix} P(y,m,d,t) \\ RP(y,m,d,t)\end{bmatrix} - S\times \dot{E}(y,m,d,t) \tag{3}$$

$$\dot{E}(y,m,d,t)=E(y,m,d,t)-E(y,m,d,t-1)-E_{stb} \tag{4}$$

The proposed MCMG is connected to the electric and natural gas upstream network. Owing to selected and installed components for the proposed MCMG, controllable or non-controllable loads need to be satisfied over the planning horizon. Electricity and heat balance in the proposed MCMG are modeled as follows, respectively:

$$\begin{aligned} &L_e(y,m,d,t)+D_e(y,m,d,t)+T_e(y,m,d,t)= \\ &+\sum_{c=1}^{Nc^{chp}} P_g(y,m,d,t)\cdot\eta_e^{chp}(c) \cdot\upsilon^{chp}(y,m,d,t)\cdot I^{chp}(c) \\ &+\sum_{c=1}^{Nc^{pv}} RP_e^{pv}(y,m,t)\cdot\eta_e^{invertor}(c)\cdot I^{pv}(c) \\ &+\sum_{c=1}^{Nc^{trans}} P_e(y,m,d,t)\cdot\eta_e^{trans}(c)\cdot I^{trans}(c) \\ &-M_e(y,m,d,t)\end{aligned} \tag{5}$$

$$\begin{aligned} &L_h(y,m,d,t)+D_h(y,m,d,t)+T_h(y,m,d,t)= \\ &+\sum_{c=1}^{Nc^{chp}} P_g(y,m,d,t)\cdot\eta_h^{chp}(c)\cdot \upsilon^{chp}(y,m,d,t)\cdot I^{chp}(c) \\ &+\sum_{c=1}^{Nc^{bo}} P_g(y,m,d,t)\cdot\eta_h^{bo}(c)\cdot\upsilon^{bo}(y,m,d,t)\cdot I^{bo}(c) \\ &-M_h(y,m,d,t)\end{aligned} \tag{6}$$

The ESS can operate as an uninterrupted energy supply system in the MCMG. With regard to the ESSs, it is assumed that the initial charge values of the storage systems are equal to its last charging cycle. Electricity and heat energy exchange (equivalent storage flows) is tackled in Eq. (7) and Eq. (8), which are directly related to storage energy derivatives, as modeled in Eq. (9) to Eq. (12).

$$M_e(y,m,d,t)=S_e(y,m,d,t)\cdot\dot{E}_e(y,m,d,t) \tag{7}$$

$$M_h(y,m,d,t)=S_h(y,m,d,t)\cdot\dot{E}_h(y,m,d,t) \tag{8}$$

$$\begin{aligned} M_e(y,m,d,t)=&\frac{1}{\eta s_e(y,m,d,t)}\cdot \\ &(E_e(y,m,d,t)-E_e(y,m,d,t-1)-E_{e,stb})\end{aligned} \tag{9}$$

$$\eta s_e(y,m,d,t)=I_e(y,m,d,t)\cdot\eta_e^{char}+\frac{\left(1-I_e(y,m,d,t)\right)}{\eta_e^{dischar}} \tag{10}$$

$$\begin{aligned} M_h(y,m,d,t)=&\frac{1}{\eta s_h(y,m,d,t)}\cdot \\ &(E_h(y,m,d,t)-E_h(y,m,d,t-1)-E_{h,stb})\end{aligned} \tag{11}$$

$$\eta s_h(y,m,d,t)=I_h(y,m,d,t)\cdot\eta_h^{char}+\frac{\left(1-I_h(y,m,d,t)\right)}{\eta_h^{dischar}} \tag{12}$$

3.2. DR program

In the future, loads will be participating in the energy market to help the management system not to fail. This means that different system policies enable the system to encourage or oblige responsive users to curtail or shift their demands to other hours (off-peak intervals) [44]. The DR programs are classified into two methods: based on price or on encouragement and penalty. In the former, the demand changes based on the energy prices in each interval. This method is used in the presented paper. Since the energy prices in the input port of the MCMG are specified while the load is supplied by different components, it is necessary to model the final energy price (FEP) of different carriers in the output port of the system. In this case, the FEPs of different carriers in the system output are determined based on input energy, component efficiency, and operation. The FEPs of carriers are modelled in Eq. (13) and Eq. (14), respectively, based on Fig.5.

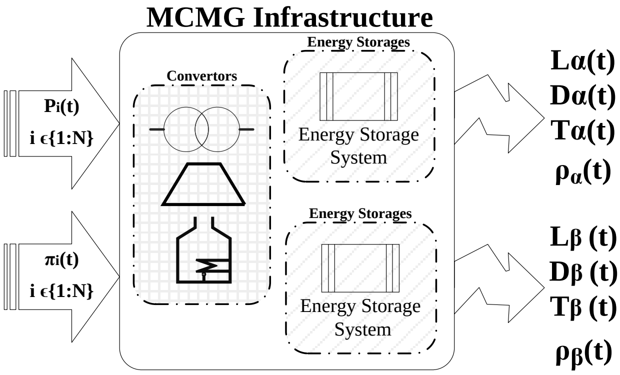

Fig. 5. Correlation between the input and output ports of carriers and their prices.

$$\rho_\alpha(t) = \frac{\sum_{i=1}^{N} P_i(t)\cdot \pi_i(t)\cdot \dfrac{\eta_{i,\alpha}}{\eta_{i,\alpha}+\eta_{i,\beta}}}{L_\alpha(t)+D_\alpha(t)+T_\alpha(t)+M_\alpha(t)} \tag{13}$$

$$\rho_\beta(t) = \frac{\sum_{i=1}^{N} P_i(t)\cdot \pi_i(t)\cdot \dfrac{\eta_{i,\beta}}{\eta_{i,\alpha}+\eta_{i,\beta}}}{L_\beta(t)+D_\beta(t)+T_\beta(t)+M_\beta(t)} \tag{14}$$

Considering the FEP for responsive loads, the elasticity matrix that indicates the load change percentage in proportion to the percentage of price changes is illustrated in Eq. (15) and Eq. (16). The diagonal elements of the mentioned matrix are positive and the others are negative—that is, with the price increasing in an hour, the responsive load would decrease and a share of the demand would be shifted to other hours.

$$.\, EL_\alpha(t,t') = \begin{pmatrix} ee_\alpha(1,1) & \cdots & ee_\alpha(1,24) \\ \vdots & \ddots & \vdots \\ ee_\alpha(24,1) & \cdots & ee_\alpha(24,24) \end{pmatrix}. \tag{15}$$

$$ee_\alpha(t,t') = \begin{cases} t = t' & ee_\alpha(t,t') \geq 0 \\ t \neq t' & ee_\alpha(t,t') < 0 \end{cases} \tag{16}$$

With regard to the definition of the elasticity matrix, the responsive demand is modelled as below:

$$D_\alpha(t) = D_{0,\alpha}(t)\cdot\left[1+\sum_{t'=1}^{24} EL_\alpha(t,t')\cdot\frac{\rho_\alpha(t)-\rho_{0,\alpha}(t')}{\rho_{0,\alpha}(t')}\right] \tag{17}$$

In Eq. (17), $D_{0,\alpha}$ is the base consumption of carrier α, which is changing in proportion to the primary price of carrier α at interval t'. The MCMG structure is modelled according to the load growth over the planning horizon and the selection of appropriate components for the proposed system. Owing to energy changes in the output port of the MCMG, the newly adjusted consumption of these responsive users and inconstant FEPs are calculated as follows:

$$D_l(y,m,d,t) = D_{0,l}(y,m,d,t) + \Delta d_l(y,m,d,t) \tag{18}$$

$$\Delta d_l(y,m,d,t) = D_{0,l}(y,m,d,t)\cdot \sum_{t'=1}^{24} EL_l(y,m,d,t,t')\cdot\frac{\Delta\rho_l(y,m,d,t')}{\rho_{0,l}(y,m,d,t')} \tag{19}$$

$$\Delta\rho_l(y,m,d,t) = \rho_l(y,m,d,t) - \rho_{0,l}(y,m,d,t) \tag{20}$$

3.3. Objective Function (OF) and Constraints

The total investment, operational, and maintenance costs are selected as the three evaluating criteria that are used as the optimal objective to be minimized in Eq. (23). The operational and maintenance costs are computed in terms of the net present value (NPV). The investment cost and operational cost (fuel and maintenance costs) are given in Eq. (24) to Eq. (26), respectively. Owing to mounted ESSs and its significant role in the proposed MCMG, the chronological load curves are used instead of the load duration curves (LDCs). The chronological load curves are obtained and considered for responsive or non-responsive loads each year based on the load-forecasting system.

$$\rho_e(y,m,d,t) = \frac{\begin{pmatrix} +\sum_{c=1}^{Nc^{trans}} P_e(y,m,d,t)\cdot\pi_e(y,m,d,t)\cdot I^{trans}(c) \\ +\sum_{c=1}^{Nc^{chp}} P_g(y,m,d,t)\cdot\upsilon^{chp}(y,m,d,t)\cdot I^{chp}(c)\cdot\pi_g(y,m,d,t)\cdot(\eta_e^{chp}(c)/\eta_e^{chp}(c)+\eta_h^{chp}(c)) \end{pmatrix}}{\begin{pmatrix} +\sum_{c=1}^{Nc^{trans}} P_e(y,m,d,t)\cdot\eta_e^{trans}(c)\cdot I^{trans}(c) + \sum_{c=1}^{Nc^{pv}} RP_e^{pv}(y,m,t)\cdot\eta_e^{invertor}(c)\cdot I^{pv}(c) \\ +\sum_{c=1}^{Nc^{chp}} P_g(y,m,d,t)\cdot\eta_e^{chp}(c)\cdot\upsilon^{chp}(y,m,d,t)\cdot I^{chp}(c) - M_e(y,m,d,t) \end{pmatrix}} \tag{21}$$

$$\rho_h(y,m,d,t) = \frac{\begin{pmatrix} +\sum_{c=1}^{Nc^{bo}} P_g(y,m,d,t)\cdot\upsilon^{bo}(y,m,d,t)\cdot\pi_g(y,m,d,t)\cdot I^{bo}(c) \\ +\sum_{c=1}^{Nc^{chp}} P_g(y,m,d,t)\cdot\upsilon^{chp}(y,m,d,t)\cdot\pi_g(y,m,d,t)\cdot I^{chp}(c)\cdot(\eta_h^{chp}(c)/\eta_h^{chp}(c)+\eta_h^{chp}(c)) \end{pmatrix}}{\begin{pmatrix} +\sum_{c=1}^{Nc^{chp}} P_g(y,m,d,t)\cdot\eta_h^{chp}(c)\cdot\upsilon^{chp}(y,m,d,t)\cdot I^{chp}(c) \\ +\sum_{c=1}^{Nc^{bo}} P_g(y,m,d,t)\cdot\eta_h^{chp}(c)\cdot\upsilon^{bo}(y,m,d,t)\cdot I^{chp}(c) - M_h(y,m,d,t) \end{pmatrix}} \tag{22}$$

$$OF = C_{inv} + C_{oper} + C_{main} \tag{23}$$

The OF equation details are as follows:

$$\begin{aligned} C_{inv} &= \sum_{c=1}^{Nc^{chp}} Invs^{chp}(c)\cdot I^{chp}(c) \\ &+ \sum_{c=1}^{Nc^{trans}} Invs^{trans}(c)\cdot I^{trans}(c) + \sum_{c=1}^{Nc^{bo}} Invs^{bo}(c)\cdot I^{bo}(c). \\ &+ \sum_{c=1}^{Nc^{pv}} Invs^{pv}(c)\cdot I^{pv}(c) \end{aligned} \tag{24}$$

$$C_{oper} = \sum_{y=1}^{Ny} \frac{1}{(1+i)^{y-1}} \cdot \sum_{m=1}^{12}\sum_{d=1}^{30}\sum_{t=1}^{24} \begin{bmatrix} +P_e(y,m,d,t)\cdot \pi_e(y,m,d,t) \\ +P_g(y,m,d,t)\cdot \pi_g(y,m,d,t) \\ -T_e(y,m,d,t)\cdot \psi_e(y,m,d,t) \\ -T_h(y,m,d,t)\cdot \psi_h(y,m,d,t) \end{bmatrix} \tag{25}$$

$$C_{main} = \sum_{y=1}^{Ny} \frac{1}{(1+i)^{y-1}} \cdot \sum_{m=1}^{12}\sum_{d=1}^{30}\sum_{t=1}^{24} \begin{bmatrix} \sum_{c=1}^{Nc^{chp}} Po_e^{chp}(y,m,d,t)\cdot K_{main}^{chp}(c)\cdot I^{chp}(c) \\ +\sum_{c=1}^{Nc^{bo}} Po_h^{bo}(y,m,d,t)\cdot K_{main}^{bo}(c)\cdot I^{bo}(c) \\ +\sum_{c=1}^{Nc^{trans}} Po_e^{trans}(y,m,d,t)\cdot K_{main}^{trans}(c)\cdot I^{trans}(c) \\ +\sum_{c=1}^{Nc^{RP}} Po_e^{pv}(y,m,t)\cdot K_{main}^{pv}(c)\cdot I^{pv}(c) \end{bmatrix} \tag{26}$$

The energy generation model by each component is formulated as follows

$$Po_e^{chp}(y,m,d,t) = \sum_{c=1}^{Nc^{chp}} P_g(y,m,d,t)\cdot \eta_e^{chp}(c)\cdot \upsilon^{chp}(t,m)\cdot I^{chp}(c) \tag{27}$$

$$Po_e^{trans}(y,m,d,t) = \sum_{c=1}^{Nc^{trans}} P_e(y,m,d,t)\cdot \eta_e^{trans}(c)\cdot I^{trans}(c) \tag{28}$$

$$Po_h^{bo}(y,m,d,t) = \sum_{c=1}^{Nc^{bo}} P_g(y,m,d,t)\cdot \eta_h^{bo}(c)\cdot \upsilon^{bo}(t,m)\cdot I^{bo}(c) \tag{29}$$

$$Po_e^{pv}(y,m,d,t) = \sum_{c=1}^{Nc^{RP}} RP_e^{pv}(y,m,d,t)\cdot \eta_e^{pv}(c)\cdot I^{pv}(c) \tag{30}$$

Owing to the capacity of each existing component, the energy generation for each convertor needs to be limited within the allowable ranges. The equality and non-equality constraints, such as the allowable range and initial values of the variables, are applied as follows:

$$\sum_{c=1}^{Nc^{chp}} \underline{Po_e^{chp}(y,m,d,t)}\cdot I^{chp}(c) \le Po_e^{chp}(y,m,d,t) \le \sum_{c=1}^{Nc^{chp}} \overline{Po_e^{chp}(y,m,d,t)}\cdot I^{chp}(c) \tag{31}$$

$$\sum_{c=1}^{Nc^{trans}} \underline{Po_e^{trans}(y,m,d,t)}\cdot I^{trans}(c) \le Po_e^{trans}(y,m,d,t) \le \sum_{c=1}^{Nc^{trans}} \overline{Po_e^{trans}(y,m,d,t)}\cdot I^{trans}(c) \tag{32}$$

$$\sum_{c=1}^{Nc^{bo}} \underline{Po_h^{bo}(y,m,d,t)}\cdot I^{bo}(c) \le Po_h^{bo}(y,m,d,t) \le \sum_{c=1}^{Nc^{bo}} \overline{Po_h^{bo}(y,m,d,t)}\cdot I^{bo}(c) \tag{33}$$

$$\sum_{c=1}^{Nc^{RP}} \underline{Po_e^{pv}(y,m,d,t)}\cdot I^{pv}(c) \le Po_e^{pv}(y,m,d,t) \le \sum_{c=1}^{Nc^{RP}} \overline{Po_e^{pv}(y,m,d,t)}\cdot I^{pv}(c) \tag{34}$$

$$\underline{E_e(y,m,d,t)} \le E_e(y,m,d,t) \le \overline{E_e(y,m,d,t)} \tag{35}$$

$$\underline{E_h(y,m,d,t)} \le E_h(y,m,d,t) \le \overline{E_h(y,m,d,t)} \tag{36}$$

$$E_e(y,m,d,1) = E_e(y,m,d,24) \tag{37}$$

$$E_h(y,m,d,1) = E_h(y,m,d,24) \tag{38}$$

$$\underline{M_e(y,m,d,t)} \le M_e(y,m,d,t) \le \overline{M_e(y,m,d,t)} \tag{39}$$

$$\underline{M_h(y,m,d,t)} \le M_h(y,m,d,t) \le \overline{M_h(y,m,d,t)} \tag{40}$$

$$\upsilon^{chp}(y,m,d,t) + \upsilon^{bo}(y,m,d,t) = 1 \tag{41}$$

$$0 \le \upsilon^{chp}(y,m,d,t) \le 1 \tag{42}$$

$$0 \le \upsilon^{bo}(y,m,d,t) \le 1 \tag{43}$$

4. Methodology

The main goal of the proposed model is to select proper appropriate components and theirs sizes by minimizing the objective function (OF) in Eq. (23) and the associated constraints. Therefore, a two-stage optimal method for solving the structural and operational problem is proposed, as shown in Fig.6. At the first stage, a genetic algorithm (GA) using MATLAB software is used to determine the appropriate components and their sizes. At the second stage, the operation and maintenance costs are simulated and calculated by the GAMS software. The manner of input data and the software performance are charted to determine the optimal design of the MCMG over the planning horizon.

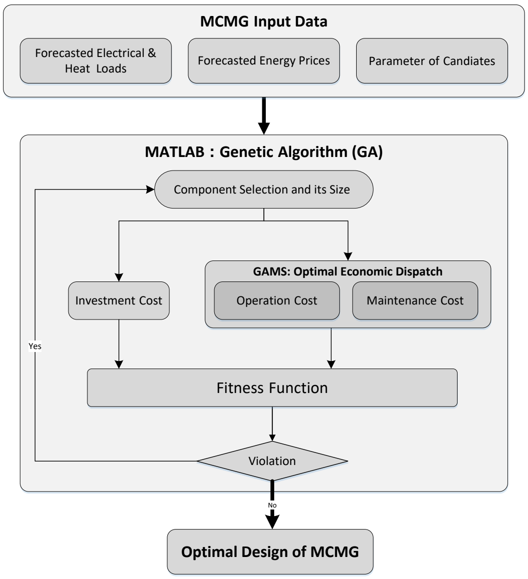

Fig. 6. Procedure of optimal planning in the network.

5. Simulation Results and Discussion

5.1. Assumptions

An MCMG is analyzed to illustrate the performance of the proposed two-stage method. A set of elements such as transformer, CHP, boiler and PV with five candidates are available to design MCMG.

The proposed MC/MG designing model has been depicted in Fig3, along with the existing electricity, natural gas, and district heat upstream networks. In order to achieve the desired MCMG performance, it is necessary to employ the optimization process. The problem is to lies in search the optimum selection of the candidates to be being placed inside the MCMG from a given set of elements to supply electricity and heat demands up to the target year (the last year of the planning horizon). A set of four elements comprise comprising of the transformer, CHP, boiler, and PV, are considered, while the energy storage system ESSs with their predetermined sizes are embedded within the network. Each generating units (elements) have has five different candidates which the candidates that are characterized by different capacities, efficiencies, investment and installation costs, and maintenance cost coefficient co-efficiency, (see Table 1). The characteristics of ESSs are stated in Table 2.

The model structure can contain either one candidate of each set, or none. Furthermore, there are no limitations on annual investments.

The planning problem is implementing a five-year planning horizon. The investment and operational costs are analyzed on an NPV basis. So, all costs are transferred to the first year using a discount rate that is assumed to be equal to the interest rate (IR) value here. The investment and installation cost is assumed to occur in the first year of the planning horizon. In addition, it is assumed that the load and energy purchase prices will be increased in future years. So, the annual load growth and energy price growth rates are considered for an operation period of five years (the fifth year is the target year), as presented in Table 3.

Table 1. Technical specification of candidates.

Element	type	Maximum capacity (KW)	Efficiencies (%)			Investment & installation cost (million $)	Maintenance coefficient ($/KWh)
			el.	th.	$\sum$		
Transformer	1	800	92		92	0.825	0.003
	2	900	90		90	1.328	0.0027
	3	1000	89		89	1.660	0.0024
	4	1500	87		87	2.490	0.0022
	5	1800	85		85	2.988	0.002
CHP	1	500	40	35	75	0.221	0.015
	2	600	40	44	84	0.272	0.0135
	3	825	50	30	80	0.375	0.0125
	4	1125	40	40	80	0.487	0.0115
	5	1350	35	40	75	0.600	0.01
Boiler	1	300		90	90	0.075	0.009
	2	450		87	87	0.1	0.008
	3	600		85	85	0.125	0.005
	4	750		83	83	0.15	0.003
	5	900		80	80	0.175	0.002
PV	1	50	90		90	0.0625	0.0017
	2	70	88		88	0.087	0.0015
	3	100	85		85	0.125	0.0014
	4	120	82		82	0.15	0.0012
	5	150	80		80	0.187	0.001

Table 2. Properties of energy storage system.

Storage elements	Charge & discharge efficiency rate (%)		Capacity (KW)	Convertor rate capacity (KWh)	
				discharging	charging
Electrical storage	95	92	90	-30	+30
Thermal storage	95	92	90	-30	+30

Table 3. Economic parameters.

Annual Interest Rate (IR) (%)	Annual load growth rate (%)	Annual energy purchasing price growth rate (%)
15	10	20

The purchase and sale prices of carriers are assumed in Fig.6. These are considered similar for each season but are increasing in each new year due to the aforementioned energy purchasing growth rate. The normalized PV generation curves for a 24-hour interval are given in Fig.7. In order to simplify and lower the computational burden of PV generation, its generation is assumed to be similar for all days in a year, though it should not have been like that due to different weather conditions, especially in summer and winter.

Each planning year is divided into 12 monthly periods, while two typical days (weekdays and weekends) of two typical seasons (summer and winter) are used to model the electric and heat demand curves are used for each season in order to lower the computational burden.

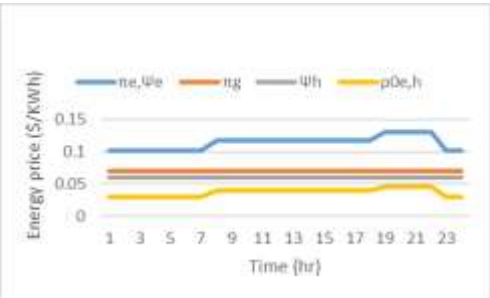

Fig. 6. Energy prices for the first year.

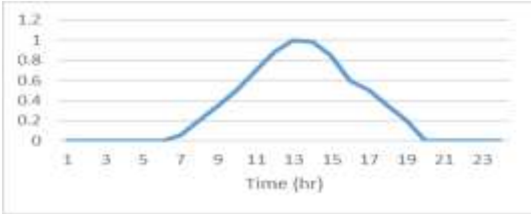

Fig. 7. The normalized PV generation curve.

5.2. Optimal Designing Results

The simulation results reveal the optimal selection and size of components in the networks that are listed in Table 4. A graphical display of the MCMG structure is depicted in Fig.8 schematically.

However, the issue is whether components are chosen optimally for efficient long-term planning of interdependent energy infrastructures. These issues can be observed in Table 1 and Table 4.

The result shows the Transformer unit type 1 has been selected because of its lower investment cost and higher efficiency compared to other units. Owing to higher electrical rather than thermal demand, the CHP unit type 3 is selected due to its high power-to-heat ratio, whereas no boiler is chosen because of the sufficient heat generation by the selected CHP. Also, the PV unit type 3 is chosen due to the zero energy-generation cost of this unit and sufficient capacity in proportion to its appropriate and rational efficiency and investment cost.

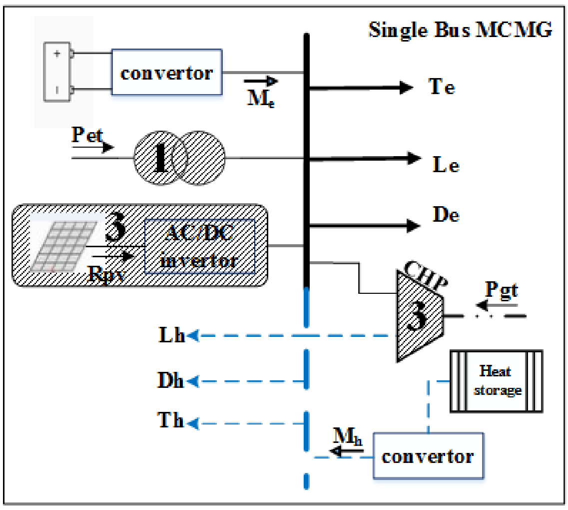

Fig. 8. MCMG design which is obtained through optimization.

Table 4. Data of selected elements.

Element	Maximum capacity (KW)	Efficiencies (%)			Investment & installation cost (million $)	Maintenance coefficient ($/KWh)
		el.	th.	$\sum$		
Transformer 1	800	92		92	0.825	0.003
CHP 3	825	50	30	80	0.375	0.0125
Boiler	-		-	-	-	-
PV 3	100	85		85	0.125	0.0014

5.3. Operational Optimization Results

In this section, the economic dispatch problem is considered in the proposed network with its chosen elements. The result of the operational optimization problem is shown in Fig.9 to Fig.15. Electrical and thermal controllable loads form a share of the total loads, as observed in Fig.9 and Fig.10, respectively. These responsive loads are encouraged or forced to shift their demand from the peak intervals to the off-peak intervals. The peak period for the electrical load is considered from Intervals 15 to 22, whereas the thermal load is in Intervals 1–7 and 23–24.

The base prices and FEPs of electricity and heat for responsive loads are acquired and depicted in Fig.11. It is observable that the FEPs of electricity and heat for responsive loads are higher than its base prices in all intervals.

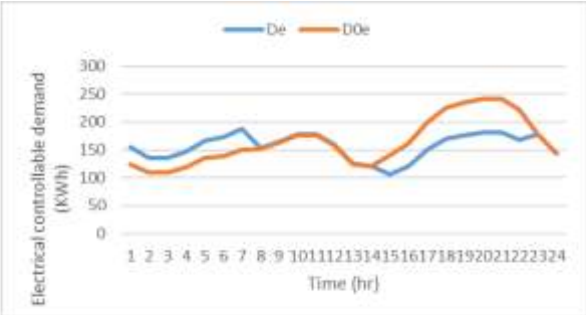

Fig. 9. Electrical responsive load profile under TOU policy for the last year of a typical weekday in winter.

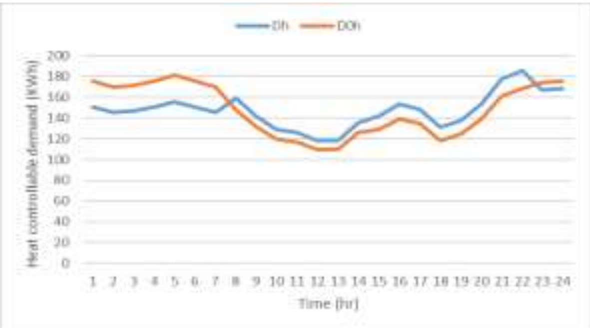

Fig. 10. Thermal responsive load profile under TOU policy for the last year of a typical weekday in winter.

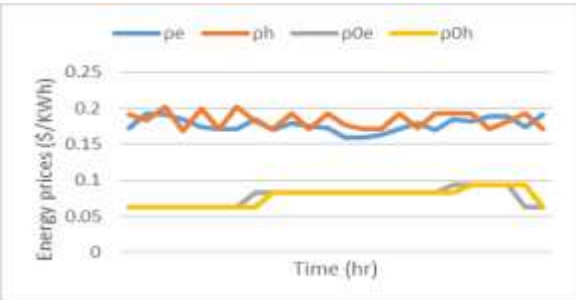

Fig. 11. Base prices and FEPs of electrical and thermal responsive loads for the last year of a typical Friday in winter.

The flexibility of the network is increased by inserting electrical and thermal storage in the designed MCMG to prevent the wastage of energies in such a way that the surplus energies resulting from distributed generations (DGs) are stored at low prices and injected back into the grid while the price is high. Moreover, the ESS provides economic benefits and improves the reliability indices for the MG [42]. The equivalent storage power flows and state of charge (SOC) of the electric and thermal storage systems are illustrated in Fig.12 and Fig.13, respectively.

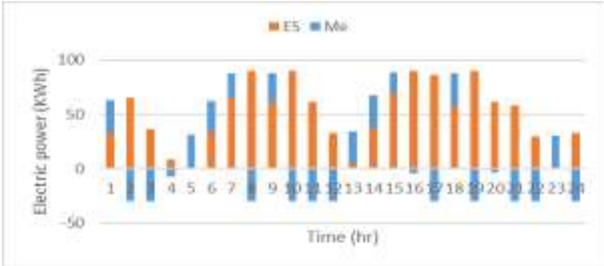

Fig. 12. Equivalent storage electricity flows and SOC of electric storage for the last year of a typical Friday in winter.

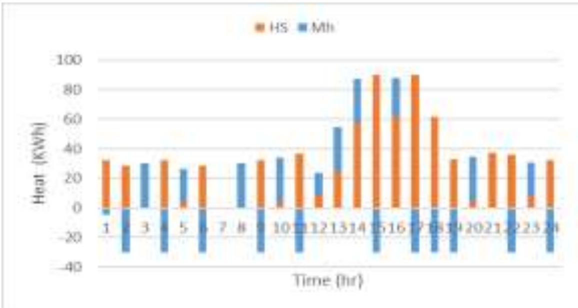

Fig. 13. Equivalent storage heat flows and SOC of thermal storage for the last year of a typical Friday in winter.

The electricity and heat balance in the designed MCMG are depicted in Fig.14 and Fig.15, respectively. On this weekday in the winter of the fifth year, the electricity purchase from the grid is equivalent to zero for all intervals while the CHP fulfils the major part of the electrical and heat demands, and sells surplus energy to the upstream network because of profitable energy trading. However, a detailed explanation of the results is difficult due to the complexity of the problem.

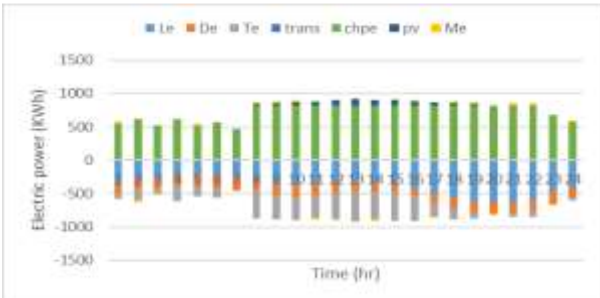

Fig. 14. Electric portion in MCMG.

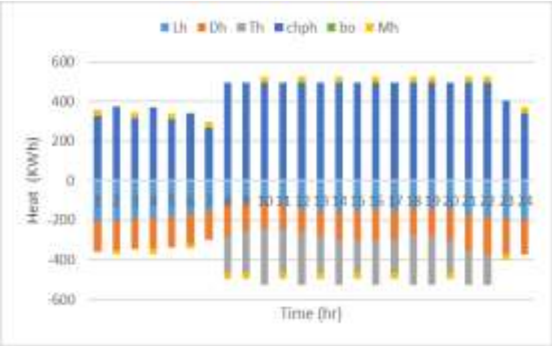

Fig. 15. Heat portion in MCMG.

Finally, the total cost of the MCMG's 24-hour operation for all planned years that are transferred to the first year and the investment cost of the selected components that are installed in the first year are listed in Table 5.

6. Conclusion

In this paper, a two-stage optimization method is used in an MCMG planning phase as well as in operation scheduling. The static planning phase determines the proper type and size of components that it would be better to install in the first year for the planning horizon, whereas the operational problem decides the optimal scheduling of the selected components, including the transformer, CHP, boiler, and PV, with the existence of ESSs and responsive loads. The total cost is the summation of investment, and the operational and maintenance costs that are transferred to the first year as the basis of the NPV. The optimization problem is modeled as an MINLP problem using the GA of MATLAB and the MINLP of the GAMS software as a compound solution method. The test case results show that the proposed model can help MCMG planners determine the most economical components along with the sizes that should be purchased and installed in order to meet multiple energy demands up to the target year. Current and future work is dedicated to model the proposed system with regard to the net zero emission (NZE) basis.

7. Abbreviations and Acronyms

Variables & parameters

Po	generated energy (KWh)
T	transferred energy (KWh)
P	received energy (KWh)
E	state of charge (storage energy) (KWh)
L	non-controllable load (KWh)
D	controllable load (KWh)
D_0	primary controllable load (KWh)
M	equivalent storage power flows (storage charge and discha
RP	renewable generation (KWh)
C	cost ($)
Invs	installation and investment cost ($)
y	year
m	month
.*t* .	time (hour)
c	Candidate No.
I	binary variable
El	elasticity
ee	elasticity element
K	coefficient
Co	convertor coupling matrix
η	efficiency

Greek signs

π	energy purchasing price ($/KWh)
ψ	energy selling price ($/KWh)
υ	dispatch factor (%)
ρ	final energy price of responsive load ($/KWh)

Superscripts

pv	photovoltaic
bo	boiler
	combined heat and power
char	charging power of storage interface
dischar	discharging power of storage interface
trans	transformer

Footnotes

e	electricity

Table 5. Total cost with and without considering NPV over the planning horizon.

<table>
<tr><th rowspan="2"></th><th colspan="4">Installation Cost of Equipment in the first year</th><th colspan="6">Operation Cost</th><th rowspan="2">Total Cost</th></tr>
<tr><th>Transformer1</th><th>CHP3</th><th>Boiler0</th><th>PV3</th><th>Year 1</th><th>Year 2</th><th>Year 3</th><th>Year 4</th><th>Year 5</th><th>All years</th></tr>
<tr><td>Cost (million $)</td><td rowspan="2">0.825</td><td rowspan="2">0.375</td><td rowspan="2">-</td><td rowspan="2">0.125</td><td>0.486</td><td>0.633</td><td>0.829</td><td>1.09</td><td>1.44</td><td>4.48</td><td></td></tr>
<tr><td>NPV Cost (million $)</td><td>0.486</td><td>0.55</td><td>0.626</td><td>0.717</td><td>0.822</td><td>3.2</td><td>4.53</td></tr>
</table>

g	natural gas
h	heat
tot	total
p	input carrier
l	output carrier
α	carriers type
0	initial (base) value
stb	standby energy losses
$invertor$	invertor
$oper$	operation
inv	investment
$main$	maintenance

References

[1] Mohsenzadeh, S. Ardalan, M.-R. Haghifam, and S. Pazouki, "Optimal place, size, and operation of combined heat and power in multi carrier energy networks considering network reliability, power loss, and voltage profile," IET Gener. Transm. Distrib., vol. 10, no. 7, pp. 1615–1621, May 2016.

[2] T. Niknam, M. Bornapour, and A. Gheisari, "Combined heat, power and hydrogen production optimal planning of fuel cell power plants in distribution networks," Energy Convers. Manag., vol. 66, pp. 11–25, 2013.

[3] C. L. M. Mago P.J., "Analysis and optimization of CCHP systems based on energy, economical, and environmental considerations," Energy Build., vol. 41, no. 10, pp. 1099–1106, 2009.

[4] A. Smith, R. Luck, and P. J. Mago, "Analysis of a combined cooling, heating, and power system model under different operating strategies with input and model data uncertainty," Energy Build., vol. 42, no. 11, pp. 2231–2240, 2010.

[5] M. Geidl, G. Koeppel, P. Favre-Perrod, B. Klöckl, G. Andersson, and K. Fröhlich, "Energy hubs for the future," IEEE Power and Energy Magazine, vol. 5, no. 1. pp. 24–30, 2007.

[6] N. Nikmehr and S. Najafi Ravadanegh, "Optimal Power Dispatch of Multi-Microgrids at Future Smart Distribution Grids," IEEE Trans. Smart Grid, vol. 6, no. 4, pp. 1648–1657, 2015.

[7] A. Nadimi and F. Adabi, "Optimized Planning for Hybrid Micro-grid in Grid-connected Mode," Int. J. Renew. Energy Res., vol. 6, no. 2, pp. 494–503, 2016.

[8] G. Andersson, "THE INFLUENCE OF COMBINED POWER, GAS, AND THERMAL NETWORKS ON THE RELIABILITY OF SUPPLY." in Proc. of 6th World Energy System Conference, Turin, Italy, 2006.

[9] L. Guo, W. Liu, J. Cai, B. Hong, and C. Wang, "A two-stage optimal planning and design method for combined cooling, heat and power microgrid system," Energy Convers. Manag., vol. 74, pp. 433–445, 2013.

[10] C. Z. Li, Y. M. Shi, and X. H. Huang, "Sensitivity analysis of energy demands on performance of CCHP system," Energy Convers. Manag., vol. 49, no. 12, pp. 3491–3497, 2008.

[11] G. Chicco and P. Mancarella, "A unified model for energy and environmental performance assessment of natural gas-fueled poly-generation systems," Energy Convers. Manag., vol. 49, no. 8, pp. 2069–2077, 2008.

[12] X. Q. Kong, R. Z. Wang, Y. Li, and X. H. Huang, "Optimal operation of a micro-combined cooling, heating and power system driven by a gas engine," Energy Convers. Manag., vol. 50, no. 3, pp. 530–538, 2009.

[13] L. Fu, X. Zhao, S. Zhang, Y. Li, Y. Jiang, H. Li, and Z. Sun, "Performance study of an innovative natural gas CHP system," in Energy Conversion and Management, 2011, vol. 52, no. 1, pp. 321–328.

[14] G. Chicco and P. Mancarella, "A comprehensive approach to the characterization of trigeneration systems," 2006.

[15] A. Shahmohammadi, M. Moradi-Dalvand, H. Ghasemi, and M. S. Ghazizadeh, "Optimal Design of Multicarrier Energy Systems Considering Reliability Constraints," IEEE Trans. Power Deliv., vol. 30, no. c, pp. 878–886, 2015.

[16] X. Zhang, M. Shahidehpour, A. Alabdulwahab, and A. Abusorrah, "Optimal Expansion Planning of Energy Hub with Multiple Energy Infrastructures," IEEE Trans. Smart Grid, vol. 6, no. 5, pp. 2302–2311, 2015.

[17] H. Seifi and M. S. Sepasian, "Electric Power System Planning: Issues, Algorithms and Solutions," Power Syst., vol. 49, 2011.

[18] W. Gu, Z. Wu, R. Bo, W. Liu, G. Zhou, W. Chen, and Z. Wu, "Modeling, planning and optimal energy management of combined cooling, heating and power microgrid: A review," Int. J. Electr. Power Energy Syst., vol. 54, pp. 26–37, 2014.

[19] D. Zhang, N. Shah, and L. G. Papageorgiou, "Efficient energy consumption and operation management in a smart building with microgrid," Energy Convers. Manag., vol. 74, pp. 209–222, 2013.

[20] S. D. Manshadi and M. E. Khodayar, "Resilient operation of multiple energy carrier microgrids," IEEE Trans. Smart Grid, vol. 6, no. 5, pp. 2283–2292, 2015.

[21] C. Unsihuay-Vila, J. W. Marangon-Lima, A. C. Z. de Souza, I. J. Perez-Arriaga, and P. P. Balestrassi, "A Model to Long-Term, Multiarea, Multistage, and Integrated Expansion Planning of Electricity and Natural Gas Systems," IEEE Trans. Power Syst., vol. 25, no. 2, pp. 1154–1168, May 2010.

[22] C. A. Saldarriaga, R. A. Hincapie, and H. Salazar, "A Holistic Approach for Planning Natural Gas and Electricity Distribution Networks," IEEE Trans. Power Syst., vol. 28, no. 4, pp. 4052–4063, Nov. 2013.

[23] M. Geidl and G. Andersson, "Optimal power flow of multiple energy carriers," IEEE Trans. Power Syst., vol. 22, no. 1, pp. 145–155, 2007.

[24] F. Kienzle, P. Favre-Perrod, M. Arnold, and G. Andersson, "Multi-energy delivery infrastructures for the future," in 2008 First International Conference on Infrastructure Systems and Services: Building Networks for a Brighter Future (INFRA), 2008, pp. 1–5.

[25] S. chandrasekaran and R. K, “Optimal Power Flow considering intermittent Wind Power using Particle Swarm optimization,” Int. J. Renew. Energy Res., vol. 6, no. 2, pp. 504–509, 2016.

[26] M. Geidl and G. Andersson, “Operational and structural optimization of multi-carrier energy systems,” in European Transactions on Electrical Power, 2006, vol. 16, no. 5, pp. 463–477.

[27] S. S, I. Gandhi, D. Samiappan, and M. M, “Security Constraint Unit Commitment on Combined Solar Thermal Generating Units Using ABC Algorithm,” Int. J. Renew. Energy Res., vol. 6, no. 4, pp. 1361–1372, 2016.

[28] F. Adamek, M. Arnold, and G. Andersson, “On decisive storage parameters for minimizing energy supply costs in multicarrier energy systems,” IEEE Trans. Sustain. Energy, vol. 5, no. 1, pp. 102–109, 2014.

[29] M. Moeini-Aghtaie, P. Dehghanian, M. Fotuhi-Firuzabad, and A. Abbaspour, “Multiagent Genetic Algorithm: An Online Probabilistic View on Economic Dispatch of Energy Hubs Constrained by Wind Availability,” IEEE Trans. Sustain. Energy, vol. 5, no. 2, pp. 699–708, Apr. 2014.

[30] J. H. Roh, M. Shahidehpour, and L. Wu, “Market-based generation and transmission planning with uncertainties,” IEEE Trans. Power Syst., vol. 24, no. 3, pp. 1587–1598, 2009.

[31] A. Sheikhi, M. S. Naderi, A. M. Ranjbar, G. B. Gharehpetian, and F. Safe, “CHP optimized selection methodology for a multi-carrier energy system,” Int. Rev. Electr. Eng., vol. 6, no. 4, pp. 1839–1846, 2011.

[32] R. Billinton and R. N. (Ronald N. Allan, Reliability evaluation of power systems. 2nd ed. New York: Plenum, 1996.

[33] A. J. del Real, A. Arce, and C. Bordons, “Optimization strategy for element sizing in hybrid power systems,” J. Power Sources, vol. 193, no. 1, pp. 315–321, 2009.

[34] S. salahi, F. adabi, and S. B. Mozafari, “Design and simulation of a hybrid micro-grid for Bisheh village,” Int. J. Renew. Energy Res., vol. 6, no. 1, pp. 199–211, 2016.

[35] G. Koeppel and G. Andersson, “Reliability modeling of multi-carrier energy systems,” Energy, vol. 34, no. 3, pp. 235–244, 2009.

[36] H. Ren and W. Gao, “A MILP model for integrated plan and evaluation of distributed energy systems,” Appl. Energy, vol. 87, no. 3, pp. 1001–1014, 2010.

[37] P. Arcuri, G. Florio, and P. Fragiacomo, “A mixed integer programming model for optimal design of trigeneration in a hospital complex,” Energy, vol. 32, no. 8, pp. 1430–1447, 2007.

[38] A. Baghernejad, M. Yaghoubi, and K. Jafarpur, “Exergoeconomic optimization and environmental analysis of a novel solar-trigeneration system for heating, cooling and power production purpose,” Sol. Energy, vol. 134, pp. 165–179, 2016.

[39] M. Geidl and G. Andersson, “Optimal coupling of energy infrastructures,” in 2007 IEEE Lausanne POWERTECH, Proceedings, 2007, pp. 1398–1403.

[40] A. Shahmohammadi, M. M. Dalvand, M. S. Ghazizadeh, and A. Salemnia, “Energy hubs’ structural and operational linear optimization with energy storage elements,” in 2011 2nd International Conference on Electric Power and Energy Conversion Systems, EPECS 2011, 2011.

[41] J. Mitra, “Reliability-based sizing of backup storage,” IEEE Trans. Power Syst., vol. 25, no. 2, pp. 1198–1199, 2010.

[42] S. Bahramirad, W. Reder, and A. Khodaei, “Reliability-Constrained Optimal Sizing of Energy Storage System in a Microgrid,” IEEE Trans. Smart Grid, vol. 3, no. 4, pp. 2056–2062, Dec. 2012.

[43] A. Sheikhi, A. M. Ranjbar, and H. Oraee, “Financial analysis and optimal size and operation for a multicarrier energy system,” Energy Build., vol. 48, pp. 71–78, 2012.

[44] W. Widayat, B. Kiono, and A. Abdullah, “Impact of Demand Side Management on Spinning Reserve Requirements Designation,” Int. J. Renew. Energy Res., vol. 7, no. 2, pp. 946–953, 2012.